

Flux jumping in thin films

R. G. Mints

*School of Physics and Astronomy, Raymond and Beverly Sackler Faculty of Exact Sciences,
Tel Aviv University, Tel Aviv 69978, Israel*

E. H. Brandt

*Institut für Physik, Max-Planck-Institut für Metallforschung, W-7000 Stuttgart 80, Germany
(Received 15 May 1996)*

The thermomagnetic flux-jump instability of the Bean critical state is considered, which may occur during flux penetration in thin films of type-II superconductors in a perpendicular magnetic field. We calculate the applied field B_j at which this instability occurs and its dependence on the ramp rate \dot{B}_a , on the nonlinear current-voltage curve, and on the thermal resistance between the film and the substrate. As examples we consider the thermomagnetic flux-jump instability at the straight edge of a superconducting film and of the same edge containing a small indentation of semicircular shape. The presence of a small indentation drastically reduces the field or ramp rate at which the thermomagnetic instability occurs. [S0163-1829(96)02938-4]

I. INTRODUCTION

Bean's critical state model¹ successfully describes the irreversible magnetization in type-II superconductors by introducing a critical current density $j_c(T, B)$ which in general depends on the temperature T and the magnetic field B . Within the Bean model in the original longitudinal geometry the slope of the stationary magnetic field profile equals $\mu_0 j_c(T, B)$ in the region where flux has penetrated. This non-uniform flux distribution is not in equilibrium, and under certain conditions a thermomagnetic flux-jump instability may arise in this critical state. The flux-jumping process results in a flux redistribution towards the equilibrium state and is accompanied by a sudden heating of the superconductor.

Flux jumping has been extensively studied in conventional and high-temperature superconductors (see the reviews in Refs. 2 and 3, references therein, and the recent experimental and theoretical studies Refs. 4–9). Two types of flux jumps can be distinguished, namely, global and local flux jumps. A *global* flux jump involves vortex motion in the entire volume of the sample. A *local* flux jump is restricted to a small fraction of the sample volume. Depending on the initial perturbation and on the driving parameters there are two qualitatively different types of global flux jumps, namely, complete and partial flux jumps. Complete jumps turn the superconductor into the normal state. Partial jumps self-terminate when the temperature is still less than the critical temperature T_c .

To illustrate the origin of a global flux jump we suppose that the temperature T_0 of the sample is increased by a small perturbation δT_0 arising due to a certain initial heat release δQ_0 . The critical current density $j_c(T)$ is a decreasing function of temperature. Thus, the density of the superconducting current screening the external magnetic field at $T = T_0 + \delta T_0$ is less than it was at $T = T_0$. This reduction of the screening current leads to a rise of the magnetic flux inside the superconductor. The resulting motion of the magnetic flux into the sample induces an additional electric field δE_0 . The perturbation δE_0 causes a further heat release

δQ_1 and temperature rise δT_1 , which reduces the superconducting screening current density j_c further. Under certain conditions this results in an avalanche-type increase of the temperature and magnetic flux in the superconductor, i.e., in a global flux jump.

The relative effect of the flux and temperature redistribution dynamics on the flux-jumping process depends on the ratio τ of the flux (t_m) and thermal (t_t) diffusion time constants.² The dimensionless parameter τ is determined by the corresponding diffusion coefficients,

$$\tau = \frac{t_m}{t_t} = \mu_0 \frac{\lambda \sigma}{C}, \quad (1)$$

where λ is the heat conductivity, σ is the electric conductivity, and C is the heat capacity.

For $\tau \ll 1$ ($t_m \ll t_t$), rapid propagation of the flux is accompanied by an adiabatic heating of the superconductor; i.e., there is not enough time to redistribute and remove the heat released due to the flux motion. For $\tau \gg 1$ ($t_t \ll t_m$), the spatial distribution of flux remains fixed during the stage of rapid heating. These adiabatic ($\tau \ll 1$) and dynamic ($\tau \gg 1$) approximations typically are used to approach the flux-jumping problem.² The flux-jump scenario significantly depends on the relation between the values of the heat conductivity λ , heat capacity C , and conductivity $\sigma(E)$ defined as the slope of the $j(E)$ curve. The dependence of σ on the electric field E (nonlinear conductivity) is an important factor determining the flux-jumping process.^{10,9} In particular, it results in the dependence of the flux-jump field B_j on the ramp rate \dot{B}_a of the external magnetic field B_a which is known from numerous experiments.^{2,3,5,8}

In the longitudinal geometry of slabs or cylinders in a parallel field, the Bean model means that the current density j can have the values 0 or j_c only. In the transverse geometry of films in a perpendicular field, one has $j = j_c$ in the regions where magnetic flux has penetrated, and a surface screening current with possible values $0 \leq j \leq j_c$ in the central flux-free region. In this central region the current density is uniform

when the film thickness d is less than the London penetration depth λ_L . For thicker films with $d \gg \lambda_L$, the screening current may be nonuniform across the thickness, forming a current-caused longitudinal Bean critical state which was recently computed.¹¹

In magnetization experiments the thermomagnetic flux-jump instability originates in the outer region where the flux has penetrated, since the electric field \mathbf{E} generated by the external magnetic field variation is maximum at the specimen edges. Computations^{12,13} show that the critical state in this penetrated region is quite similar for the longitudinal and transverse limits $d \rightarrow \infty$ and $d \rightarrow 0$. In particular, in these two limits the spatial distributions of \mathbf{j} and \mathbf{E} are very similar. Indeed, when complete penetration is reached these two geometries even exhibit identical current density and electric field profiles. This finding allows one to use the expressions for the field \mathbf{E} of the longitudinal limit as good approximations for thin films in a perpendicular field. We note for completeness that the magnetic field profiles are rather different in these two geometries.^{1,11-16}

The presence of edge defects strongly modifies the flow of the currents in the film and significantly affects the electric field generated in the flux penetration process. In particular, calculations as well as a simple estimate show that a small indentation with a semicircular edge drastically enhances the value of E in the vicinity of this edge defect.^{17,12,18} The enhancement of electric field in the presence of the edge defects is specific for the longitudinal geometry and can influence the critical state stability in thin films.

Let us estimate the electric field occurring in typical magnetization experiments. The external magnetic field ramp rate \dot{B}_a is usually in the interval $\dot{B}_a < 1 \text{ T s}^{-1}$. The electric field E generated by the magnetic field variation is of the order of $E \sim \dot{B}_a x_p$, where x_p is the flux penetration depth. To estimate the field E we use $x_p < 10^{-4} \text{ m}$ which results in $E < 10^{-6} \text{ V cm}^{-1}$. This electric field interval corresponds to the flux creep regime with the dependence of j on E taking the form

$$j(E) = j_c + j_1 \ln\left(\frac{E}{E_0}\right), \quad (2)$$

where E_0 is the voltage criterion at which the critical current density j_c is defined, j_1 determines the slope of the $j(E)$ curve, and $j_1 \ll j_c$. The actual choice of E_0 is not crucial. Indeed, by choosing for the voltage criterion a certain value \tilde{E}_0 instead of E_0 we change the critical current density from j_c to $\tilde{j}_c = j_c - j_1 \ln(\tilde{E}_0/E_0)$. The difference between \tilde{j}_c and j_c is small since $\ln(\tilde{E}_0/E_0) \sim 1$ and $j_1 \ll j_c$. It is common to define j_c as the current density at which $E_0 = 10^{-6} \text{ V cm}^{-1}$.

The j - E curve in the flux creep regime is often described as a power law,

$$j(E) = j_c \left(\frac{E}{E_0}\right)^{1/n}, \quad (3)$$

with $n \gg 1$. Expanding this into a series in $1/n \ll 1$ and keeping the first two terms, we find that if we take $n = j_c/j_1$, then Eqs. (2) and (3) coincide with an accuracy of $1/n^2 \ll 1$.

The relation given by Eq. (2) was first derived in the framework of the Anderson-Kim model¹⁹⁻²¹ which considers the thermally activated uncorrelated hopping of bundles of vortices. The vortex-glass²² and collective creep^{23,24} models result in more sophisticated dependences of j on E . However, these $j(E)$ curves closely coincide with Eq. (2) if $j - j_c \ll j_c$. The recently developed self-organized criticality approach to the critical state^{25,26} also results in Eq. (2) if $j - j_c \ll j_c$. The logarithmic dependence of the current density j on the electric field E in the interval $j - j_c \ll j_c$ is in good agreement with numerous experimental data.²⁷

Equation (2) yields the conductivity

$$\sigma = \sigma(E) = \frac{dj}{dE} = \frac{j_1}{E}. \quad (4)$$

We estimate this as $\sigma > 10^{10} \text{ } \Omega^{-1} \text{ cm}^{-1}$ using the typical data $j_1 > 10^3 \text{ A cm}^{-2}$ and $E < 10^{-7} \text{ V cm}^{-1}$. It follows from this estimate that the conductivity σ determining the flux-jump dynamics for magnetization experiments is very high. As a consequence the dimensionless ratio τ is also very high. Thus, the scenario of a flux jump for the magnetization experiments corresponds to the limiting case when $\tau \gg 1$ and the initial rapid heating stage of a flux jump takes place on the background of a ‘‘frozen-in’’ magnetic flux.

In this paper we consider the thermomagnetic flux-jump instability of the Bean critical state during flux penetration into a thin film, which generates the background of a non-uniform electric field. We find the flux-jump field B_j and its dependence on the external magnetic field ramp rate \dot{B}_a and the thermal resistance between the film and the substrate. The general results are applied to consider the critical state stability in a thin film with a straight edge without and with a small indentation.

The organization of this paper is as follows. In Sec. II, we derive a general criterion for the onset of thermomagnetic instability flux jump in a superconducting film. In Sec. III this criterion is applied to calculate the flux-jump field for a thin film with a straight edge without and with a small semicircular indentation. Section IV discusses these results.

II. STABILITY CRITERION

In this section we treat the stability of the critical state assuming that the thermomagnetic flux-jump instability develops much faster than the magnetic flux diffusion process.

Let us consider a superconducting film of thickness d subjected to a magnetic field \mathbf{B}_a perpendicular to the film (xy plane). Now suppose that the temperature of the sample T_0 is increased by a small perturbation δT . To keep the critical state stable, i.e., to keep the screening current at the same level, an electric field perturbation δE arises. The additional electric field δE causes an additional heat release $\delta Q \propto \delta E$, which is the ‘‘price’’ for keeping the screening current density at the same level.

The critical state is stable if the additional heat release δQ can be removed by the additional heat flux δW resulting from the temperature perturbation δT . The temperature dynamics follows from the heat diffusion equation

$$C \frac{\partial T}{\partial t} = \lambda \Delta T + \mathbf{jE}. \quad (5)$$

Let us now consider a film which is in a thermal contact with the substrate (plane $z=0$). We characterize the thermal resistance of this contact by a heat transfer coefficient h and neglect the heat flux to the coolant (plane $z=d$). In this case the temperature perturbation satisfies the boundary conditions $\lambda \delta T'(x,y,0) = h \delta T(x,y,0)$ and $\delta T'(x,y,d) = 0$, where the prime denotes the derivative with respect to z .

To derive the explicit form of this stability criterion we need the relation between δT and δE . To obtain this, we calculate the decrease of the current density δj_- resulting from a temperature perturbation δT and the increase of the current density δj_+ resulting from an electric field perturbation δE . If the critical state is stable, the total screening current density stays constant. Thus the relation between δE and θ follows from

$$\delta j = \delta j_- + \delta j_+ = 0. \quad (6)$$

In the critical state one has $j \approx j_c$ and the decrease of j due to the temperature perturbation θ is

$$\delta j_- = - \left| \frac{\partial j_c}{\partial T} \right| \delta T \quad (7)$$

(note that $\partial j_c / \partial T < 0$). The increase of the current density due to the electric field perturbation δE is

$$\delta j_+ = \frac{dj}{dE} \delta E = \sigma \delta E. \quad (8)$$

Combining Eqs. (4) and (8) we find the relation between δj_+ and δE in the form

$$\delta j_+ = \frac{j_1}{E_b} \delta E = \frac{j_c}{nE_b} \delta E, \quad (9)$$

where $n = j_c / j_1 \gg 1$. From Eqs. (6), (7), and (9) then follows that

$$\delta E = \frac{1}{\sigma} \left| \frac{\partial j_c}{\partial T} \right| \delta T = \frac{nE_b}{j_c} \left| \frac{\partial j_c}{\partial T} \right| \delta T. \quad (10)$$

Equations (4) and (10) allow us to understand the effect of the background electric field E_b on the critical state stability. From Eq. (4) we see that a low-background electric field E_b results in a high differential conductivity $\sigma \propto 1/E_b$. In its turn this high conductivity σ leads to a small electric field perturbation since Eq. (10) states that $\delta E \propto 1/\sigma \propto E_b$. The smaller is δE , the less ‘‘costly’’ it is to remove the additional heat release. As a result, the lower is the background electric field E_b during creep, the more stable is the superconducting state.

We write the temperature as $T = T_0 + \delta T \exp(\gamma t)$ and use Eqs. (5) and (10) to find an equation for δT ,

$$\gamma C \delta T = \lambda \Delta \delta T + nE_b \left| \frac{\partial j_c}{\partial T} \right| \delta T. \quad (11)$$

The rate γ characterizes the time development of the instability. If $\gamma > 0$, any perturbation of the temperature will increase; i.e., the stability margin corresponds to $\gamma = 0$.

In the case of a thin film the background electric field is a function of x and y only. One can thus separate the variables in the heat diffusion equation and the function $\delta T(x,y,z)$ matching the boundary conditions at $z=0, d$ takes the form

$$\delta T = \theta(x,y) \left(\cos qz + \frac{h}{\lambda q} \sin qz \right), \quad (12)$$

where q is determined by the equation

$$\tan qd = \frac{h}{\lambda q}. \quad (13)$$

In particular, it follows from Eq. (13) that in the case of an ideal thermal contact ($h \rightarrow \infty$) $q^2 \approx \pi^2/4d^2$ and in the case of a high thermal boundary resistance ($hd \ll \lambda$) $q^2 \approx h/\lambda d$.

Substituting Eq. (12) into Eq. (11) we find that the stability margin is determined by the existence of a nontrivial solution of the equation

$$\Delta_{\perp} \theta - q^2 \theta + \frac{nE_b}{\lambda} \left| \frac{\partial j_c}{\partial T} \right| \theta = 0, \quad (14)$$

with the boundary condition $\mathbf{n} \nabla \theta = 0$ at the edge of the film, where \mathbf{n} is the unit vector perpendicular to the edge of the film in the film plane.

The eigenvalue equation (14) has the form of the Schrödinger equation of quantum mechanics. It means, in particular, that the variational method²⁸ can be used to determine the lowest eigenvalue (‘‘energy’’) q_{\min}^2 and eigenfunction (‘‘wave function’’) $\theta(x,y)$ by minimizing the energy functional $\mathcal{E}[\theta(x,y)]$ with respect to the parameters a_1, a_2, \dots of some trial function $\theta(x,y,a_1,a_2,\dots)$, where

$$\mathcal{E}[\theta(x,y)] = \frac{\int \theta'^2 dx dy - \alpha \int E_b \theta^2 dx dy}{\int \theta^2 dx dy} \quad (15)$$

and

$$\alpha = \frac{n}{\lambda} \left| \frac{\partial j_c}{\partial T} \right|. \quad (16)$$

III. EXAMPLES

To fix ideas we consider two examples, the long straight edge of a superconducting film of rectangular shape and the same edge with a small semicircular indentation. We will see that this indentation drastically enhances the electric field induced during flux penetration. At this little defect the thermomagnetic flux-jump instability originates thus at much lower values of the applied field than at a flawless edge. In both cases we approximate the film by a superconducting half plane $y \geq 0$ and assume the film thickness d to be much smaller than all other relevant lengths of this problem.

The background electric field $\mathbf{E}_b(x,y)$ follows from Faraday’s law $\text{rot} \mathbf{E}_b = -\dot{\mathbf{B}}$ with appropriate boundary conditions.

In the fully penetrated state the current density has saturated; therefore, the current-caused part of the induction $\mathbf{B}(x, y)$ does not change with time when the applied field B_a is further increased. One thus has $\text{rot}\mathbf{E}_b = -\dot{\mathbf{B}}_a$. The resulting $\mathbf{E}_b(x, y)$ in the critical state crucially depends on the specimen shape as discussed in detail in Ref. 12. For partial penetration one has in longitudinal geometry for the half space $y \geq 0$ the current density $\mathbf{j} = \mathbf{e}_x j(y)$ with $j(y) = j_c$ for $0 \leq y \leq y_p$ and $j(y) = 0$ for $y > y_p$, where $y_p = B_a / \mu_0 j_c$ is the penetration depth. The background electric field in this case is $\mathbf{E}_b = \mathbf{e}_x E_b(y)$ with

$$E_b(y) = \begin{cases} \dot{B}_a(y_p - y) & \text{for } 0 \leq y \leq y_p, \\ 0 & \text{for } y \geq y_p. \end{cases} \quad (17)$$

In particular, $\max\{E_b(y)\} = \dot{B}_a B_a / \mu_0 j_c$ occurs at the edge $y = 0$. The background electric field (17) is a good approximation also for thin films.^{11,13} Inserting Eq. (17) into Eq. (14) we obtain

$$\theta''(y) + c_1(y_p - y)\vartheta(y_p - y)\theta(y) = q^2\theta(y), \quad (18)$$

where $\vartheta(\xi) = 0$ for $\xi < 0$, $\vartheta(\xi) = 1$ for $\xi \geq 0$, and

$$c_1 = \frac{n\dot{B}_a}{\lambda} \left| \frac{\partial j_c}{\partial T} \right|. \quad (19)$$

Before we solve the eigenvalue equation (18) we note that from physical reasons we expect that the instability originates at the film edge where $E_b(y)$, Eq. (17), is maximum. We further expect that the heat flows mainly along z , into the substrate, and much less heat flows along x and y . This means that in Eqs. (14) and (18) one should have $|\nabla^2\theta| \ll q^2\theta$. Therefore, the criterion for thermomagnetic flux-jump instability may be found by equating in Eq. (18) the heat production term at the edge, $c_1 y_p \theta(0)$, to the heat sink term $q^2 \theta(0)$. This yields the criterion for flux jumping at the straight edges of films, $c_1 y_p = q^2$. Using the expressions for c_1 and y_p we present it as

$$\frac{c_1 y_p}{q^2} = \frac{B_j \dot{B}_a n}{\mu_0 \lambda q^2 j_c} \left| \frac{\partial j_c}{\partial T} \right| = 1. \quad (20)$$

The stability criterion (20) determines the flux-jump field B_j at the straight edges and in particular the dependence of B_j on the external magnetic field ramp rate \dot{B}_a and the heat transfer coefficient h from the film to the substrate.

We shall use now Eq. (18) to estimate the width a of the eigenfunction $\theta(y)$, i.e., the extension of the heated region at the onset of flux jumping. Our above considerations assume that this width is wider than the film thickness but still narrower than the penetration depth y_p , $d \ll a \ll y_p$. This is indeed the case, as we can easily estimate by a variational method.²⁸ With a simple Gaussian trial function $\theta = \exp(-y^2/2a^2)$ the integrals in Eq. (15) are easily evaluated, and minimization with respect to a yields the stability criterion (20) and the width

$$a = \pi^{1/6} c_1^{-1/3} = \pi^{1/6} \left(\frac{y_p}{q^2} \right)^{1/3}. \quad (21)$$

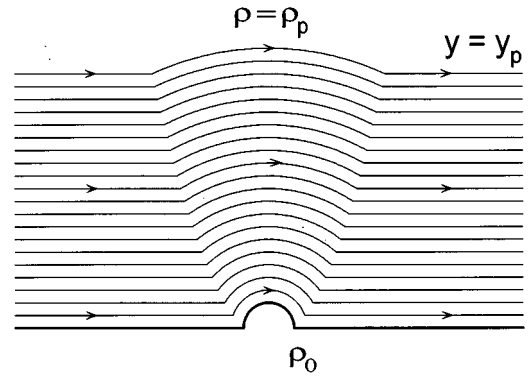


FIG. 1. A film with an indentation in the form of a semicircle with radius ρ_0 and centered at $x=y=0$. The straight and circular lines are the field lines of the current density \mathbf{j} and electric field \mathbf{E} (in the film plane) during penetration of magnetic flux.

For the second equality we used the criterion $c_1 y_p = q^2$, Eq. (20). Assuming that $q y_p \gg 1$ we find, from Eq. (21), $d \ll a \ll y_p$, which was required for the criterion (20). Note that the condition $q y_p \gg 1$ leads to $y_p \gg d$ for the case of an ideal thermal contact between the film and the substrate and to $y_p \gg \sqrt{\lambda/hd}$ for the case of a high thermal boundary resistance.

As a second example we consider the same straight film edge $y=0$ but with a small indentation with a semicircular edge, $x^2 + y^2 = \rho_0^2$, $y \geq 0$. The radius ρ_0 of this defect should be larger than the film thickness d and much smaller than the penetration depth $y_p \approx B_j / \mu_0 j_c$ at which the instability occurs, $d \ll \rho_0 \ll y_p$. The presence of this indentation strongly modifies the flow of the critical currents and drastically enhances the background electric field which is induced during flux penetration by the moving vortex lines.^{17,12,18}

The current stream lines first are parallel to the edge $y=0$, then the current flows on circles concentric with the defect (centered at $x=y=0$), and then flows again parallel to $y=0$; cf. Fig. 1. The straight and circular flows are separated by the parabola $y = (x^2 - \rho_0^2) / 2\rho_0$. This current density \mathbf{j} has the same orientation as the electric field \mathbf{E}_b . However, the magnitudes j and E_b exhibit different behavior: While $j = j_c$ is constant in the considered penetrated region, E_b is sharply peaked at the indentation and decreases monotonically to zero as it approached the front line $y_{\text{front}}(x)$. Beyond the flux front one has $j = E_b = B = 0$. For longitudinal geometry, the exact shape of the front line is known, $y_{\text{front}}(x) = \max[y_p, (\rho_p^2 - x^2)^{1/2}]$, with $\rho_p = \rho_0 + y_p$. This longitudinal result may be used as an approximation for the film, as is confirmed by computations.¹¹⁻¹³ Inside the region of circular flow the conditions $\text{rot}\mathbf{E}_b = -\dot{\mathbf{B}}_a$ and $E_b = 0$ at $\rho = \sqrt{x^2 + y^2} = \rho_p$ are satisfied by the solution

$$\mathbf{E}_b = \mathbf{e}_\varphi \frac{\dot{B}_a}{2} \left(\frac{\rho_p^2}{\rho} - \rho \right). \quad (22)$$

The irrotational $1/\rho$ term in Eq. (22) means a pronounced enhancement of the background electric field near small indentations. The height of this maximum is

$\max\{E_b(\rho)\} \approx \dot{B}_a \rho_p^2 / 2\rho_0$, which is higher than the maximum field $\dot{B}_a y_p$, Eq. (17), at the defect-free edge by a factor $y_p / 2\rho_0 \gg 1$.

We expect the thermomagnetic flux-jump instability to originate at the position of maximum E_b , i.e., at the edge $\rho = \rho_0$ of the indentation. As for the defect-free edge, we will find that the width a of the nucleus $\theta(\rho)$ is much smaller than the penetration depth $\rho_p \approx y_p$ and even smaller than the defect radius ρ_0 . The curvature of the indentation may thus be disregarded. Expanding $E_b(\rho)$ with respect to $(\rho - \rho_0) / \rho_p \ll 1$ and keeping only the constant and linear terms, we obtain $E_b(\rho) = \frac{1}{2} \dot{B}_a (\rho_p / \rho_0)^2 [\rho_0 - (\rho - \rho_0)]$. The resulting eigenvalue equation has thus the same form as Eq. (18) if one makes the replacements $y \rightarrow \rho - \rho_0$, $y_p \rightarrow \rho_0$, and $c_1 \rightarrow c_2$ with

$$c_2 = \frac{\dot{B}_a \rho_p^2 n}{2 \rho_0^2 \lambda} \left| \frac{\partial j_c}{\partial T} \right| \quad (23)$$

and $\rho_p \approx B_j / \mu_0 j_c$. The stability criterion for flux jumping at a small indentation of radius ρ_0 is thus $c_2 \rho_0 = q^2$. Using Eq. (23) we present it as

$$\frac{c_2 \rho_0}{q^2} = \frac{B_j^2 \dot{B}_a n}{2 \mu_0^2 \lambda q^2 \rho_0 j_c^2} \left| \frac{\partial j_c}{\partial T} \right| = 1. \quad (24)$$

The stability criterion (24) determines the flux-jump field B_j at a small indentation and in particular the dependence of B_j on the external magnetic field ramp rate \dot{B}_a , the indentation radius ρ_0 , and the heat transfer coefficient h from the film to the substrate.

Using the same replacement as above we find that the trial function $\theta = \exp[-(\rho - \rho_0)^2 / 2a^2]$ has the width

$$a = \pi^{1/6} c_2^{-1/3} = \pi^{1/6} \left(\frac{\rho_0}{q^2} \right)^{1/3}. \quad (25)$$

Assuming that $q y_p \gg 1$ we find $d \ll a \ll \rho_0$; i.e., the thermomagnetic flux-jump instability originates only in a narrow band at the curved edge of the indentation.

IV. CONCLUSIONS

Comparing the criteria (20) and (24) for the onset of thermomagnetic flux-jump instability at the straight edge of a film with and without indentation, one finds that the factor $c_1 y_p$ in Eq. (20) is replaced by $c_2 \rho_0$, where $c_2 \approx c_1 y_p^2 / 2\rho_0^2$. Thus the ramp rate \dot{B}_a at which a flux jump occurs at a given flux-jump field B_j is smaller for the indentation by a factor $2\rho_0 / y_p \approx 2\rho_0 \mu_0 j_c / B_a \ll 1$. At a constant ramp rate the instability occurs at a smaller field B_j when the film edge exhibits an indentation. It follows also from Eqs. (20) and (24) that at a straight edge $B_j \propto \dot{B}_a^{-1}$ and at a small indentation $B_j \propto \dot{B}_a^{-1/2}$.

To fix ideas we consider the example of a rather thick film, $d = 100 \mu\text{m}$, $\rho_0 = 200 \mu\text{m}$, $j_c = 10^9 \text{ A/m}^2$, $j_c / |\partial j_c / \partial T| = 10 \text{ K}$, $n = 50$, and $\lambda = 0.1 \text{ W/K m}$. Using Eqs. (24) and (13) we find for $h \geq 10^3 \text{ W/K m}^2$ the estimate $B_j \approx \dot{B}_a^{-1/2}$ where the units are tesla for B_j and T/s for \dot{B}_a . Thus even in a thick film the flux-jump instability occurs at rather high fields. In particular, this estimate results in $B_j = 10 \text{ T}$ for $\dot{B}_a = 10^{-2} \text{ T/s}$ and in $B_j = 1 \text{ T}$ for $\dot{B}_a = 1 \text{ T/s}$.

This example reveals that in much thinner films thermomagnetic flux jumping is not to be expected within the range of fields and ramp rates occurring in typical experiments or applications of superconducting films. Clearly, the reason for this stability of the critical state is the effective cooling of a thin film on a substrate. If desired, the parameters of an experiment may be chosen such that the predicted flux-jump instability should occur. But note that for very large applied fields the penetration depth $\rho_p \approx B_a / \mu_0 j_c$ formally will be larger than the half width a of the film; in this case one has to put $\rho_p = a$ in c_2 , Eq. (23). Further increase of B_a above the field of full penetration $B_p = \mu_0 j_c a$ will then not lead to flux jumping since the electric field has saturated to a final profile even as the current density.

ACKNOWLEDGMENTS

We acknowledge support from the German-Israeli Foundation for Research and Development, Grant No. 1-300-101.07/93.

¹C.P. Bean, Phys. Rev. Lett. **8**, 250 (1962); Rev. Mod. Phys. **36**, 31 (1964).

²R.G. Mints and A.L. Rakhmanov, Rev. Mod. Phys. **53**, 551 (1981).

³S.L. Wipf, Cryogenics **31**, 936 (1991).

⁴M.E. McHenry, H.S. Lessure, M.P. Maley, J.Y. Coulter, I. Tanaka, and H. Kojima, Physica C **190**, 403 (1992).

⁵L. Legrand, I. Rosenman, Ch. Simon, and G. Collin, Physica C **211**, 239 (1993).

⁶A. Gerber, J.N. Li, Z. Tarnawski, J.J.M. Franse, and A.A. Menovsky, Phys. Rev. B **47**, 6047 (1993).

⁷P. Leiderer, J. Boneberg, P. Brüll, V. Bujok, and S. Herminghaus, Phys. Rev. Lett. **71**, 2646 (1993).

⁸L. Legrand, I. Rosenman, R.G. Mints, G. Collin, and E. Janod, Europhys. Lett. **34**, 287 (1996).

⁹R.G. Mints, Phys. Rev. B **53**, 12 311 (1996).

¹⁰R.G. Mints and A.L. Rakhmanov, J. Phys. D **15**, 2297 (1982).

¹¹E.H. Brandt, Phys. Rev. B (to be published); Phys. Rev. Lett. **76**, 4030 (1996).

¹²E.H. Brandt, Phys. Rev. B **52**, 15 442 (1995); Rep. Prog. Phys. **58**, 1465 (1995).

¹³Th. Schuster, H. Kuhn, E.H. Brandt, M.V. Indenbom, M. Leghissa, M. Kraus, M. Kläser, G. Müller-Vogt, H.-U. Habermeier, H. Kronmüller, and A. Forkl, Phys. Rev. B **52**, 10 375 (1995).

¹⁴P.N. Mikheenko and Yu.E. Kuzovlev, Physica C **204**, 229 (1993).

¹⁵E.H. Brandt, M.V. Indenbom, and A. Forkl, Europhys. Lett. **22**, 735 (1993); E.H. Brandt and M.V. Indenbom, Phys. Rev. B **48**, 12 893 (1993).

¹⁶E. Zeldov, J.R. Clem, M. McElfresh, and M. Darwin, Phys. Rev. B **49**, 9802 (1994).

¹⁷A.M. Campbell and J.E. Evetts, Adv. Phys. **72**, 199 (1972).

¹⁸Th. Schuster, M.V. Indenbom, M.R. Koblischka, H. Kuhn, and H. Kronmüller, Phys. Rev. B **49**, 3443 (1994).

- ¹⁹P.W. Anderson, Phys. Rev. Lett. **9**, 309 (1962).
- ²⁰Y.B. Kim, C. Hempstead, and A. Strnad, Phys. Rev. Lett. **9**, 306 (1962); Phys. Rev. **131**, 2484 (1963).
- ²¹P.W. Anderson and Y.B. Kim, Rev. Mod. Phys. **36**, 39 (1964).
- ²²M.P.A. Fisher, Phys. Rev. Lett. **61**, 1415 (1989); D.S. Fisher, M.P.A. Fisher, and D.A. Huse, Phys. Rev. B **43**, 130 (1991).
- ²³M.V. Feigelman, V.B. Geshkenbein, A.I. Larkin, and V.M. Vinokur, Phys. Rev. Lett. **63**, 2303 (1989).
- ²⁴T. Nattermann, Phys. Rev. Lett. **64**, 2454 (1990); K.H. Fisher and T. Nattermann, Phys. Rev. B **43**, 10 372 (1991).
- ²⁵Z. Wang and D. Shi, Solid State Commun. **90**, 405 (1994).
- ²⁶W. Pan and S. Doniach, Phys. Rev. B **49**, 1192 (1994).
- ²⁷See A. Gurevich and H. Küpfer, Phys. Rev. B **48**, 6477 (1993) and references therein.
- ²⁸L.D. Landau and E.M. Lifshitz, *Quantum Mechanics* (Pergamon Press, Oxford, 1991), p. 58.